Property-Driven Development of Metallic Structural Materials by Combinatorial Techniques on the Example of Fe–C–Cr Steels

Christian Baron* and Hauke Springer

The use of high-throughput techniques allows for rapid property-driven materials development. Attractive material profiles are systematically screened and processed on the example of the ternary Fe–C–Cr system into yet unexplored regions. The effect of various combinations of Cr additions (2, 4, 6, 8, 10 wt%) on the mechanical properties and microstructures of Fe–0.2C (wt%) and Fe–0.8C (wt%)-based steels are studied depending on their hardening (850–1150 °C; 20 min) and tempering conditions (100–600 °C; 1 h), producing 120 different material states. Wide ranges of potentially interesting material profiles are obtained with strengths up to 1.8 GPa ultimate tensile strength (UTS) or hardness of 700 HV5. Individual trends for materials' mechanical performance are identified, but straightforward interpretation of trends holds complex multidimensional analytical challenges of this high-throughput bulk metallurgical screening. Methods addressing these problems are outlined and the possibilities of assistive computational data processing and analysis are discussed.

1. Introduction

Fe–C–Cr-based steels represent one of the largest classes of metallic structural materials, due to their huge range of property profiles achievable by different thermo-mechanical treatments and alloy compositions.[1] The addition of C allows to increase the strength of Fe via the formation of Fe_3C carbide (cementite), which can be obtained in a variety of morphologies and dimensions, from micrometric eutectoid lamellae in pearlite down to nanoscaled precipitates within bainite. C can also be brought into solid solution at elevated temperature within austenite, from where rapid cooling leads to the transformation of extremely hard martensite. Adding Cr to Fe–C steels leads to the formation of alloy carbides with different stoichiometry and crystal structure, such as hexagonal M_7C_3 and cubic face-centered $M_{23}C_6$.

Dr. C. Baron, Dr. H. Springer
Department Microstructure Physics and Alloy Design
Max-Planck-Institut für Eisenforschung GmbH
Düsseldorf 40237, Germany
E-mail: c.baron@mpie.de

The ORCID identification number(s) for the author(s) of this article can be found under https://doi.org/10.1002/srin.201900404.

Furthermore, Cr substantially lowers the critical cooling velocity of martensitic steels (increasing hardenability), lowers the martensite start temperature, and effectively increases the corrosion resistance.[2,3] As shown in **Figure 1**, the coupled effects of various combinations of C/Cr additions have been exploited in a plethora of widely applied steel grades, from construction to bearing, hot-working, tool, and stainless steels.[2–4] Their respective compositions (which of course comprise additional elements such as Mn, Si, or Mo) and processing regimes are constantly being refined to increase their respective property profile. The development of steels has to strike a complex balance though, to avoid simply improving one property at the loss of another, such as in the classic trade-off between strength and ductility.[5] Consequently, it requires deep understanding of the complex relationships between alloy/processing, microstructure, and properties. Therefore, the currently produced and applied steel grades are often the result of decades, if not centuries, of iterative development.[6]

The systematic analysis of Figure 1 also reveals large areas of C/Cr combinations which are not yet utilized for commercially available steels, namely, medium Cr concentrations between 2 and 10 wt% for lower (about 0.2 wt%) and higher (about 0.8 wt%) C contents. At first glance, there appears to be no particular reason why no attractive property profiles would be achievable in this composition range, especially in view of the wide range of applicable heat-treatment parameters. One example for such a successful departure from the beaten path of steel development is the work of Yuan et al.[7] Here, an unconventional heat treatment for a tool steel (0.45 wt% C and 13.5 wt% Cr) leads to properties extremely favorable, for example, for automotive applications: By choosing an unusually high austenitization temperature, formation of nanoscaled reverted austenite could occur during subsequent tempering, yielding a strength in excess of 2 GPa at a tensile ductility of more than 10%.[7] Despite these appealing results—especially, as they were possible even in such a long-researched alloy system—the aforementioned iterative development strategy, often relying on the linear expansion of known relationships, typically renders such findings as surprises and accidental.

Switching from the knowledge-based expansion to a systematic screening of the yet-unexplored regions of the Fe–C–Cr alloy system might also reveal attractive property profiles; not necessarily
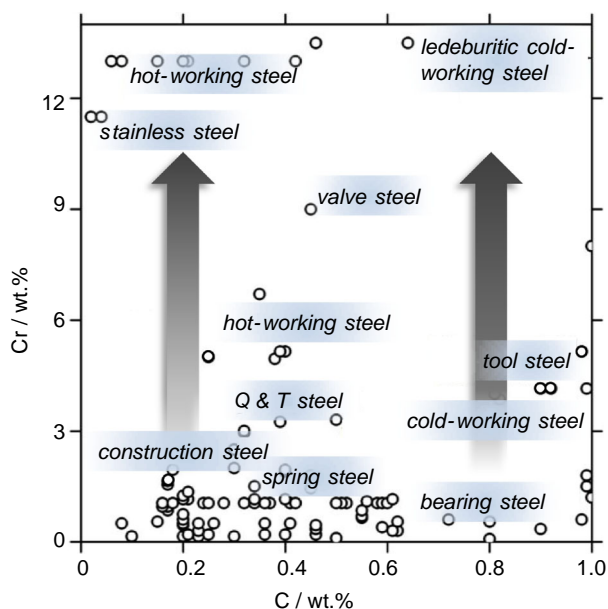
Figure 1. Simplified overview and summary plot of a plethora of various steels categorized by their applications based on their C and Cr contents.[2–4] The gray arrows indicate the little investigated compositional ranges covered in this study.

for maximum strength at sufficient ductility required for automotive body structures as in the aforementioned example but also for other applications such as energy conversion or construction engineering. However, the conventional experimental approaches for such an undertaking are typically too slow or costly, and purely theory-based material development has not fully matured yet. Such a systematic screening is, therefore, a prime example for recently introduced bulk combinatorial techniques. The rapid alloy prototyping (RAP) methodology, for example, has already been successfully introduced and utilized for various alloy systems.[8–11] Here, we demonstrate our RAP results for the areas of the Fe–C–Cr system that is yet to be explored. Rather than expecting immediate success in finding revolutionary property profiles, we aim at disseminating yet unknown material data. In addition to providing the base for further analysis and steel development, we utilize our findings to exemplify the associated analytical challenges of high-throughput bulk metallurgical screening procedures based on substantial practical experience, and discuss their effects on material design strategies.

2. Experimental Section

2.1. Synthesis and Processing

Alloy compositions and heat treatments were chosen using an integrated software-assisted approach based on thermodynamic calculations (Thermo-Calc 2015a; database TCFE7). Compositions are given throughout the article in wt%. The equilibrium phase diagrams of the two alloy concepts investigated: 1) Fe–0.2C–XCr and 2) Fe–0.8C–XCr ($X = 2$, 4, 6, 8, 10) are both plotted in **Figure 2** in a simplified form (temperature on y-axis;
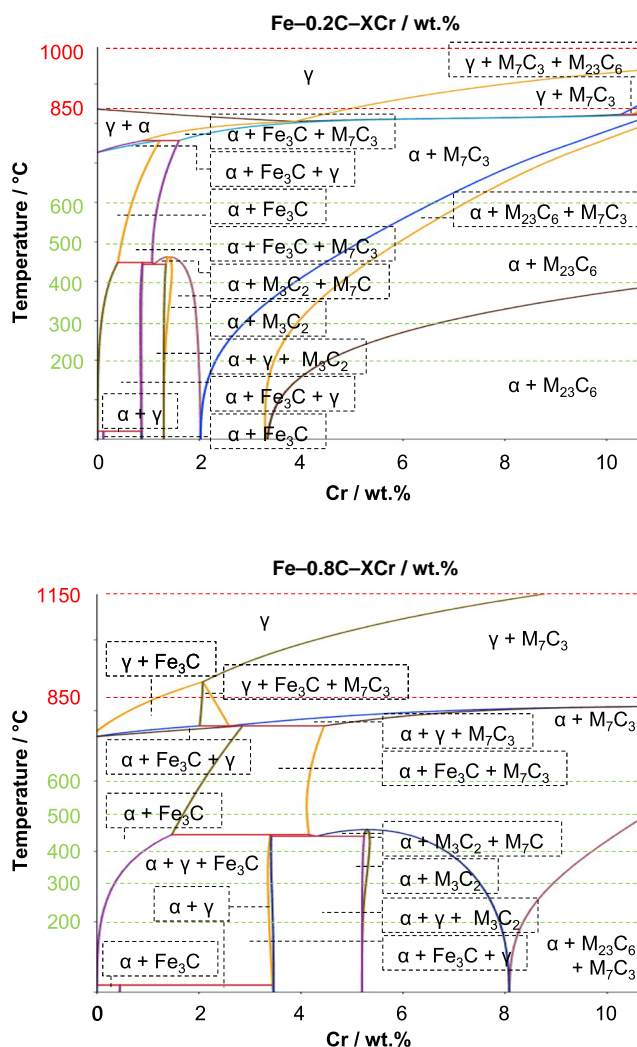
Figure 2. Equilibrium phase diagrams of the two-alloy concepts investigated based on thermodynamic calculations (Thermo-Calc 2015a; database TCFE7). Hardening temperatures are exemplarily shown by the red dashed lines; tempering temperatures are shown by the green dashed lines.

Cr content on x-axis). Alloys were produced and processed by multiple runs of the RAP method.[8–11] After melting in a vacuum induction furnace and casting into rectangular Cu-molds, samples were subsequently hot-rolled in multiple passes at 1000 °C (alloys 1) and 1150 °C (alloys 2) from 10 to 2 mm thickness. After the final rolling pass sheets were reheated and held for 5 min at rolling temperature and oil-quenched to room temperature (RT), the sheets were cut in 50 mm long pieces each for heat treatments. Temperatures applied in heat treatments are exemplarily indicated by the dashed lines in Figure 2; red for hardening temperatures and green for tempering temperatures. Hardening treatments were conducted by annealing the alloys 1) at 850 and 1000 °C and alloys 2) at 850 and 1150 °C, respectively, for 10 min in air, followed by oil-quenching to RT. Tempering was carried out by annealing for 1 h at 200, 300, 400, 500, and 600 °C (in air, oil-quenching to RT). All alloys are referred to by their aforementioned target compositions in wt%.

**ADVANCED
SCIENCE NEWS**

www.advancedsciencenews.com

**steel
research**
international

www.steel-research.de

Table 1. Target and actual chemical compositions (wt%) determined by wet chemical analyses of all alloys of this study (Fe as balance).

Target values [wt%]	Actual values [wt%]
Fe–0.2C–2Cr	Fe–0.20C–(2.1–2.2)Cr
Fe–0.2C–4Cr	Fe–(0.18–0.22)C–(4.1–4.2)Cr
Fe–0.2C–6Cr	Fe–(0.18–0.24)C–(6.1–6.2)Cr
Fe–0.2C–8Cr	Fe–(0.17)C–(8.0–8.1)Cr
Fe–0.2C–10Cr	Fe–(0.15–0.19)C–(10.1–10.2)Cr
Fe–0.8C–2Cr	Fe–0.80C–(2.1–2.2)Cr
Fe–0.8C–4Cr	Fe–(0.80–0.83)C–(4.0–4.1)Cr
Fe–0.8C–6Cr	Fe–(0.8–0.85)C–6.1Cr
Fe–0.8C–8Cr	Fe–(0.78–0.81)C–(8.0–8.1)Cr
Fe–0.8C–10Cr	Fe–(0.83–0.84)C–(10.1)Cr

The actual compositions determined by wet chemical analysis are listed in **Table 1**.

2.2. Characterization and Testing

The mechanical properties of the different alloys were probed by tensile testing. Therefore, sheets were sand-blasted with fine grit at low pressure to remove oxide scales and tensile specimens (dogbone shaped flat samples; gauge length 20 mm) cut by spark erosion. Testing was conducted with an initial strain rate of $10^{-3}\,\mathrm{s}^{-1}$ on a conventional tensile testing machine (Zwick/Roell RetroLine Z100) equipped with hydraulic gripping and laser extensometer. Macro-hardness measurements (Vickers Hardness, HV5) were conducted using a conventional Vickers hardness tester (Zwick/ZHV 10) on the outer surface (rolling plane) of the heads of the tested tensile samples after grinding to 400 grit. Tensile values represent average data of three measurements and hardness values of five measurements for every condition. Microstructural characterization was performed on cross-sections of the heads of the tested tensile samples taken perpendicular to the rolling direction. Surfaces were prepared by grinding, polishing, and etching using standard metallographic techniques. Microstructure characterization was performed by scanning electron microscopy (SEM; Zeiss Merlin) in backscatter-electron (BSE) mode. Phase indication was performed on polished samples via electron backscatter diffraction (EBSD) analysis (OIM software v.7; 0.10 µm step size) on areas of $50 \times 150\,\mu\mathrm{m}^2$ or larger, and X-ray diffraction (XRD; Seifert Type ID-3003, Meteor 0D – energy dispersive point detector, beam diameter 1.5 mm). The phases were quantified and fractions determined by Rietveld analyses of the XRD spectra (database Bruker Topas V5.0 software).

3. Results

3.1. Mechanical Characterization

Totally 120 different material conditions were studied. The mechanical properties (mean average values of total 360 tensile tests and 600 hardness measurements) for the 1) Fe–0.2C–XCr and 2) Fe–0.8C–XCr ($X = 2, 4, 6, 8, 10$) alloys are plotted

exemplarily in **Figure 3** and **4**, respectively. Here, the following material parameters are plotted: a) the yield strength (YS), b) ultimate tensile strength (UTS), c) total elongation (TE), and d) Vickers hardness (HV5). In both cases, the filled squares represent the values determined from samples treated at the lower upstream hardening temperature, whereas unfilled squares represent the higher upstream hardening temperatures. The individual material parameters determined for all material states analyzed are listed in (**Table 2**).

3.1.1. Fe–0.2C–XCr Alloys

All alloys hardened and tempered Fe–0.2C based alloys (Figure 3) exhibit an increase in strength up to several hundred MPa from 2 Cr to 4 Cr. The strength levels often seem to increase or saturate with increasing Cr concentration. Greatest YS increase was found for the material hardened at 850 °C (filled symbols; YS 2Cr: 1100 MPa; YS 4Cr: 1350 MPa), followed by a constant YS decrease with increasing Cr content, yielding about 1175 MPa (10 Cr material) in the same state. Identical trend can be observed for the UTS. It is noticeable that decrease in strength can only be observed for alloys hardened at 850 °C (unfilled green symbols), whereas the strength of the alloys hardened at 1000 °C (filled green symbols) remains almost constant after the first described rise. Interestingly, a conspicuous YS drop of about 200 MPa can be noted between 6 Cr and 8 Cr hardened at 1000 °C and annealed at 400 °C (unfilled blue rectangles). The lowered YS also remains constant for the 10 Cr alloy. The strength levels (YS/UTS) tend to decrease with increasing tempering temperatures—even though not linear—independent from the hardening treatment, down to 600–700 MPa for high tempering temperatures (600 °C). While ductility increases typically with increasing Cr content, materials maintain sufficient ductility even for low Cr contents (around 6–8% TE for the 2 Cr alloyed material) albeit low tempering temperatures after hardening. No premature embrittlement was obtained. Materials tempered at 600 °C reveal highest TE around 15%. The hardness values tend to increase with increasing Cr concentration. The values start around (300–350 HV5), followed by a rise up to additional 100 HV5. Materials tempered at 600 °C reveal significantly lower hardness values ranging from 200 HV5 up to 250 HV5.

3.1.2. Fe–0.8C–XCr Alloys

Hardened Fe–0.8C based materials (Figure 4) reveal extremely brittle behavior during tensile testing (premature failure at low strains despite high inherent strength). In some cases, it was not possible to determine any values, e.g., for some alloys hardened at 850 °C. Interestingly, low-temperature tempering (200 °C) did not affect the ductility of the alloys hardened at 1150 °C, whereas the alloys tempered at 850 °C seem to become more ductile with increasing Cr content (yielding in up to 4% TE for the 10 Cr alloyed material). Higher tempering temperatures typically translate into not only higher TE values, yielding in up to 12% TE for the 10 Cr alloy hardened at 850 °C and tempered at 600 °C (filled cyan symbols), but also rather lower hardness values around 300 HV5 independent from the Cr alloying content.

Fe–0.2C–XCr / wt.%

Figure 3. Color-coded plots of selected material parameters (YS, UTS, TE, Hardness) for the different Fe-based alloys inhering 0.2 C and diverging Cr content in different material states (filled symbols: hardened at 850 °C and tempered; unfilled symbols: hardened at 1150 °C and tempered).

Highest hardness values conversely (up to 670 HV5) were obtained for the 2 Cr alloy hardened at 850 °C and tempered at 500 °C, followed by a constant decrease with increasing Cr content. This value was found to be higher than those obtained for the hardened states. Values measured for all other states independent from the Cr alloying content are oscillating around 450–500 HV5.

3.2. In-Depth Microstructural Characterization

Microstructure characterization results for the Fe–0.2C–4Cr (left) and Fe–0.2C–8Cr (right) alloys quenched from 1000 °C and tempered at 400 °C (both oil-quenched) are compiled in **Figure 5** cross-sections; SEM SE mode). The SE images (top) reveals a lath-shaped microstructure for both the alloys, confirmed by the EBSD image quality data map (middle) in gray scale superimposed with the phases Fe α (red). XRD results (bottom, black line) are plotted together with the fitting results of the indicated phases. For both alloys, the fitting results indicated α′ (red), whereas only the 8 Cr alloy seems to inhere fractions of $M_{23}C_6$ (blue) carbides. The austenite phase seems to be absent.

4. Discussion

4.1. Microstructure/Property Relationship

We observed independent from the tempering treatment of Fe–0.2C based alloys a strength increase (YS and UTS) from 2 Cr to 4 Cr additions (Figure 3). Both most likely inhere high fractions of lath martensite, reaching strengths higher than 1000 N mm^{-2}, which is typically obtained in low-carbon steels.[12,13] The different strength levels may possibly be attributed to phenomena such as increased carbide precipitation or solid solution hardening induced by the increased Cr addition.[2,3,14–17] The evaluation of hardened and as-quenched states (black rectangles; Figure 3) show disparate behavior with increasing Cr content. Considering that hardening temperatures were deliberately chosen to provoke miscellaneous material behavior, it suggests itself that multiple phase regimes are crossed for the lower hardening temperature, i.e., full γ and combinations with M_7C_3. Diverging phase constitutions, e.g., various γ fractions prior to testing may be accountable for the increased ductility obtained with increasing Cr content (Figure 3).[18] Considering the tempering treatments, interpretation of diverging material behavior becomes even more complex and requires in-depth analysis to verify the microstructural
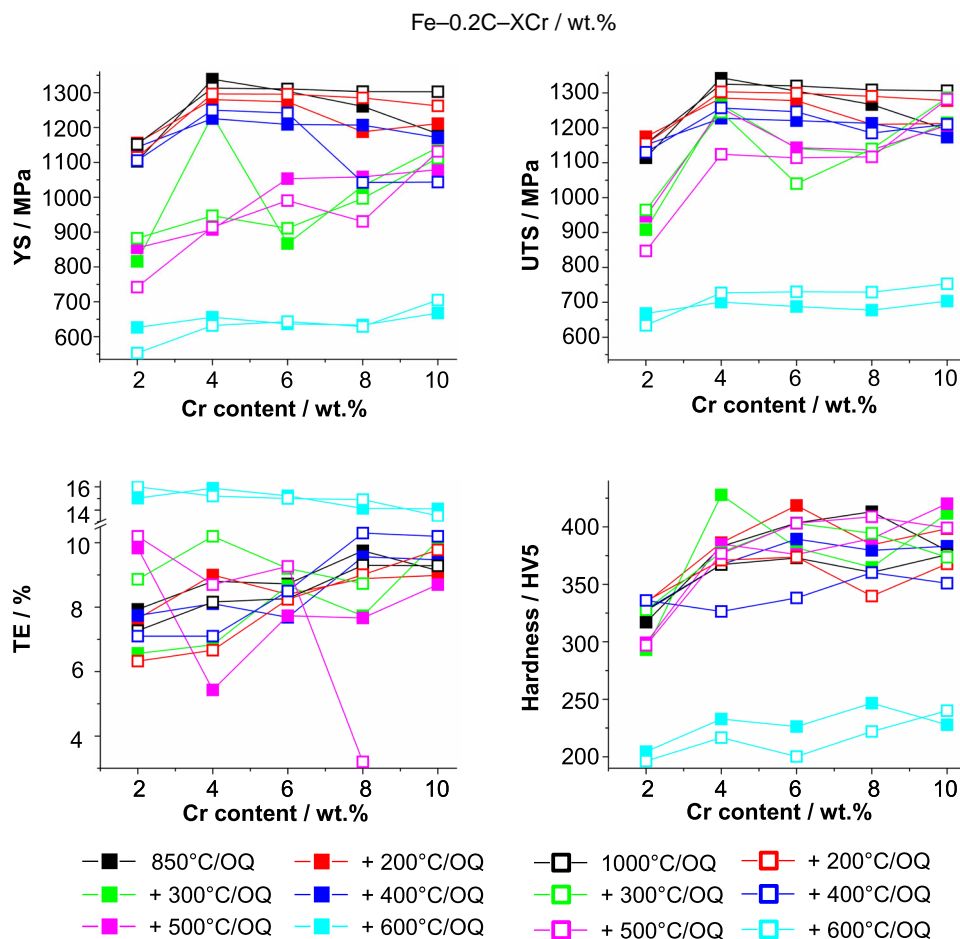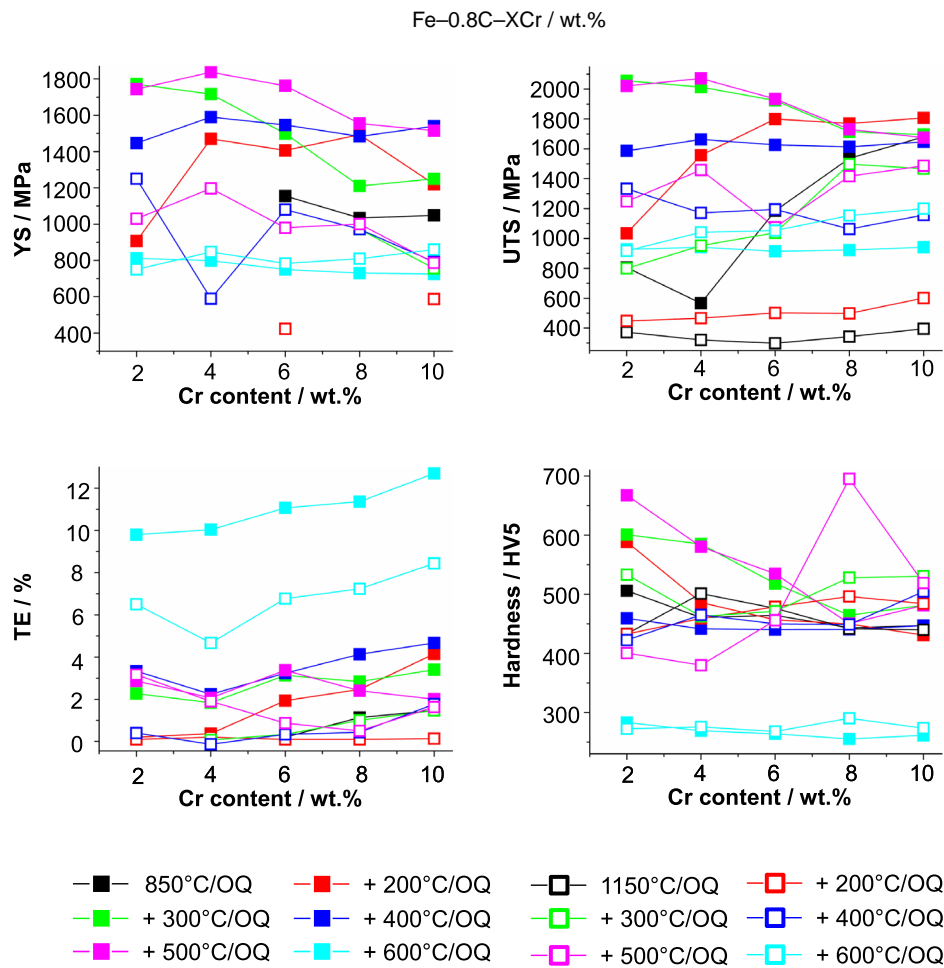
Figure 4. Color-coded plots of selected material parameters (YS, UTS, TE, Hardness) for the different Fe-based alloys inhering 0.8 C and diverging Cr content in different material states (filled symbols: hardened at 850 °C and tempered; unfilled symbols: hardened at 1150 °C and tempered).

Table 2. Material parameters (TE, YS, UTS, HV5) for the different hardening and tempering conditions of all material states analyzed in this study.

		TE	TE mean	YS	YS mean	Rm	Rm mean	HV5_1	HV5_2	HV5_3	HV5_4	HV5_5	HV5 mean
Fe–0.2C–X													
10 min @ 850 °C/OQ	2 Cr	7.7	**7.9**	1034	**1103**	1034	**1114**	282	254	309	372	366	**317**
		9.4		1130		1136							
		6.7		1144		1172							
	4 Cr	8.5	**8.8**	1316	**1339**	1328	**1344**	377	371	387	394	386	**383**
		8.5		1323		1323							
		9.4		1378		1380							
	6 Cr	9.0	**8.7**	1326	**1304**	1330	**1305**	394	412	403	400	408	**403**
		8.7		1294		1294							
		8.5		1292		1292							
	8 Cr	9.7	**9.8**	1257	**1261**	1264	**1267**	407	401	410	428	420	**413**
		10.6		1252		1259							
		9.0		1273		1277							
	10 Cr	10.1	**9.1**	1177	**1182**	1189	**1194**	368	381	378	388	382	**379**
		6.9		1180		1184							
		10.5		1189		1210							

Table 2. Continued.

		TE	TE mean	YS	YS mean	Rm	Rm mean	HV5_1	HV5_2	HV5_3	HV5_4	HV5_5	HV5 mean
10 min @ 850 °C/OQ	2 Cr	6.7	**7.6**	1168	**1156**	1221	**1174**	270	382	294	358	364	**334**
1 h @ 200 °C/OQ		8.1		1065		1066							
		8.1		1234		1236							
	4 Cr	8.9	**9.0**	1290	**1280**	1291	**1285**	373	390	368	384	416	**386**
		9.3		1232		1241							
		8.8		1318		1324							
	6 Cr	7.7	**8.4**	1274	**1274**	1280	**1278**	414	404	441	412	422	**419**
		8.5		1280		1280							
		9.0		1267		1273							
	8 Cr	7.3	**8.9**	1102	**1188**	1146	**1210**	383	373	400	386	380	**384**
		9.9		1238		1250							
		9.5		1224		1233							
	10 Cr	9.1	**9.0**	1210	**1211**	1211	**1212**	384	398	424	380	406	**398**
		9.2		1210		1210							
		8.7		1213		1215							
10 min @ 850 °C/OQ	2 Cr	0.6	**6.6**	870	**816**	938	**908**	278	292	286	307	302	**293**
1 h @ 300 °C/OQ		8		822		933							
		11.1		756		854							
	4 Cr	4.7	**6.8**	1235	**1235**	1245	**1266**	415	438	419	443	424	**428**
		7.6		1207		1283							
		8.2		1262		1270							
	6 Cr	10	**8.7**	1018	**867**	1188	**1141**	379	392	403	361	374	**382**
		9.9		879		1184							
		6.1		704		1050							
	8 Cr	8.2	**7.7**	1007	**1033**	1158	**1127**	360	310	402	377	375	**365**
		8.8		1041		1108							
		6.2		1049		1116							
	10 Cr	10.1	**10.1**	1201	**1142**	1221	**1214**	401	402	406	408	441	**412**
		9.8		1168		1198							
		10.3		1059		1224							
10 min @ 850 °C/OQ	2 Cr	8.4	**7.7**	1106	**1144**	1106	**1151**	375	307	346	308	304	**328**
1 h @ 400 °C/OQ		7.9		1169		1169							
		6.9		1157		1178							
	4 Cr	8.5	**8.1**	1240	**1226**	1244	**1227**	379	423	336	366	332	**367**
		6.9		1225		1225							
		9.0		1213		1213							
	6 Cr	7.4	**7.7**	1194	**1209**	1216	**1221**	373	403	339	422	410	**389**
		7.5		1213		1222							
		8.1		1220		1224							
	8 Cr	9.7	**9.6**	1212	**1207**	1215	**1213**	387	382	375	374	380	**380**
		9.9		1203		1213							
		9.2		1206		1210							
	10 Cr	8.8	**9.5**	1179	**1171**	1180	**1173**	394	390	384	376	372	**383**
		9.5		1167		1167							
		10.2		1167		1173							

Table 2. Continued.

		TE	TE mean	YS	YS mean	Rm	Rm mean	HV5_1	HV5_2	HV5_3	HV5_4	HV5_5	HV5 mean
10 min @ 850 °C/OQ	2 Cr	10.2	**9.8**	888	**855**	960	**946**	292	284	297	317	306	**299**
1 h @ 500 °C/OQ		8.2		867		961							
		11.1		809		918							
	4 Cr	7.1	**5.4**	536	**908**	1268	**1256**	393	404	393	375	360	**385**
		2.3		1069		1257							
		6.9		1117		1245							
	6 Cr	10.7	**7.7**	1027	**1053**	1179	**1143**	381	360	359	387	393	**376**
		7.7		1111		1168							
		4.8		1022		1081							
	8 Cr	6.7	**7.7**	987	**1058**	1101	**1137**	385	374	370	407	413	**390**
		7.4		1095		1162							
		8.9		1093		1147							
	10 Cr	8.6	**8.7**	1092	**1079**	1198	**1207**	449	443	366	431	412	**420**
		8.3		1039		1209							
		9.2		1106		1215							
10 min @ 850 °C/OQ	2 Cr	14.8	**15.0**	623	**626**	666	**668**	208	199	210	205	200	**204**
1 h @ 600 °C/OQ		15.5		612		663							
		14.8		645		675							
	4 Cr	15.8	**15.9**	667	**656**	717	**700**	231	237	235	229	232	**233**
		16.1		656		697							
		15.7		644		688							
	6 Cr	15.0	**15.2**	633	**637**	688	**688**	228	217	224	230	232	**226**
		15.5		631		694							
		15.1		646		682							
	8 Cr	16.4	**14.1**	642	**633**	686	**677**	240	253	241	250	249	**247**
		11.9		629		669							
		14.1		629		677							
	10 Cr	14.1	**14.1**	666	**668**	703	**703**	239	231	220	221	228	**228**
		14.8		657		705							
		13.4		680		702							
10 min @ 1000 °C/OQ	2 Cr	7.1	**7.3**	1148	**1152**	1149	**1155**	344	323	313	330	325	**327**
		7.8		1146		1153							
		6.9		1162		1163							
	4 Cr	8.1	**8.2**	1312	**1313**	1324	**1325**	371	366	365	360	374	**367**
		8.5		1320		1341							
		7.8		1306		1310							
	6 Cr	7.6	**8.3**	1318	**1311**	1320	**1320**	378	363	382	372	370	**373**
		8.8		1313		1330							
		8.4		1301		1310							
	8 Cr	8.8	**9.3**	1304	**1303**	1305	**1309**	326	384	370	352	370	**360**
		9.7		1310		1316							
		9.4		1296		1305							
	10 Cr	9.5	**9.3**	1305	**1303**	1308	**1306**	388	356	369	372	394	**376**
		9.9		1300		1307							
		8.4		1304		1304							

Table 2. Continued.

		TE	TE mean	YS	YS mean	Rm	Rm mean	HV5_1	HV5_2	HV5_3	HV5_4	HV5_5	HV5 mean
10 min @ 1000 °C/OQ	2 Cr	6.3	**6.3**	1054	**1115**	1105	**1154**	350	320	363	316	328	**335**
1 h @ 200 °C/OQ		7.0		1192		1196							
		5.8		1098		1161							
	4 Cr	6.5	**6.7**	1283	**1296**	1302	**1303**	360	408	363	358	366	**371**
		6.8		1308		1309							
		6.8		1298		1299							
	6 Cr	9.1	**8.2**	1296	**1296**	1297	**1299**	372	352	384	379	382	**374**
		7.0		1289		1297							
		8.6		1302		1304							
	8 Cr	9.3	**9.0**	1296	**1285**	1296	**1290**	353	271	359	361	355	**340**
		8.9		1277		1290							
		8.9		1283		1285							
	10 Cr	10.3	**9.8**	1238	**1262**	1277	**1278**	363	365	391	359	361	**368**
		9.9		1280		1287							
		9.2		1269		1270							
10 min @ 1000 °C/OQ	2 Cr	6.2	**8.9**	916	**882**	916	**965**	312	327	317	337	346	**328**
1 h @ 300 °C/OQ		10.1		848		1004							
		10.3		883		974							
	4 Cr	10.6	**10.2**	1172	**947**	1273	**1245**	381	389	378	385	357	**378**
		9.7		1019		1232							
		10.3		649		1230							
	6 Cr	10.4	**9.2**	913	**911**	1092	**1040**	397	395	402	419	402	**403**
		9.4		977		1095							
		7.8		843		933							
	8 Cr	11.6	**8.7**	941	**997**	1108	**1139**	424	403	373	386	386	**394**
		9.4		1024		1157							
		5.2		1025		1153							
	10 Cr	10.2	**10.6**	1264	**1113**	1287	**1286**	386	404	387	337	354	**374**
		10.2		962		1285							
		11.4		1111		1287							
10 min @ 1000 °C/OQ	2 Cr	7.8	**7.1**	1144	**1105**	1144	**1130**	327	343	347	335	327	**336**
1 h @ 400 °C/OQ		5.7		1044		1118							
		7.7		1127		1127							
	4 Cr	7.1	**7.1**	1247	**1250**	1250	**1257**	337	348	342	293	312	**326**
		7.2		1247		1263							
		7.0		1255		1256							
	6 Cr	9.2	**8.5**	1272	**1242**	1272	**1246**	327	378	230	373	383	**338**
		8.2		1197		1208							
		8.2		1257		1257							
	8 Cr	10.3	**10.3**	1000	**1042**	1222.58	**1185**	376	382	303	369	371	**360**
				988		1159							
				1139		1172							
	10 Cr	9.6	**10.2**	1160	**1044**	1220	**1210**	347	363	256	387	402	**351**
		10.8		927		1200							

Table 2. Continued.

		TE	TE mean	YS	YS mean	Rm	Rm mean	HV5_1	HV5_2	HV5_3	HV5_4	HV5_5	HV5 mean
10 min @ 1000°C/OQ	2 Cr	10.6	**10.2**	688	**742**	879	**847**	297	290	302	299	297	**297**
1 h @ 500°C/OQ		9.7		727		800							
		10.3		812		863							
	4 Cr	7.5	**8.7**	1054	**914**	1099	**1124**	355	384	360	408	377	**377**
		8.4		997		1153							
		10.2		691		1121							
	6 Cr	4.4	**9.3**	968	**990**	1055	**1114**	404	394	394	418	406	**403**
		11.3		1006		1135							
		12.1		997		1153							
	8 Cr	1.2	**3.2**	994	**931**	1112	**1117**	421	419	419	393	392	**409**
		0		867		1123							
		8.4				1115							
	10 Cr	14.2	**10.5**	1179	**1132**	1285	**1282**	415	356	413	404	408	**399**
		6.3		1199		1284							
		11.1		1017		1277							
10 min @ 1000°C/OQ	2 Cr	16	**16.0**	553	**553**	634	**634**	174	200	206	201	200	**196**
1 h @ 600°C/OQ	4 Cr	15.2	**15.2**	632	**632**	727	**727**	224	212	219	198	230	**217**
	6 Cr	15	**15.0**	643	**643**	730	**730**	183	164	210	219	225	**200**
	8 Cr	14.9	**14.9**	629	**629**	729	**729**	219	216	223	230	222	**222**
	10 Cr	13.5	**13.5**	705	**705**	753	**753**	238	235	248	233	244	**240**
Fe–0.8C–X													
10 min @ 850°C/OQ	2 Cr	0.2	**0.10**	788	**788**	855	**805**	519	529	454	497	530	**506**
		0.1				936							
		0				625							
	4 Cr					497	**566**	474	469	456	442	461	**460**
						731							
						470							
	6 Cr	0.1	**0.20**		**1155**		**1185**	461	454	466	458	482	**464**
		0.2		1160		1170							
		0.3		1150		1200							
	8 Cr	0.8	**1.13**	1070	**1034**	1520	**1536**	467	447	430	430	442	**443**
		0.7		1070		1370							
		1.9		961		1720							
	10 Cr	1.7	**1.47**	1010	**1048**	1690	**1680**	423	464	456	463	429	**447**
		0.9		1140		1580							
		1.8		995		1770							
10 min @ 850°C/OQ	2 Cr	0.4	**0.20**	1270	**907**	1330	**1035**	647	636	597	567	495	**588**
1 h @ 200°C/OQ		0		543		1050							
						725							
	4 Cr	−0.1	**0.37**		**1470**	1540	**1556**	496	443	482	488	521	**486**
		−0.1				1400							
		1.3		1470		1730							
	6 Cr	2.3	**1.93**	1350	**1407**	1870	**1800**	483	471	438	453	438	**457**
		1.9		1430		1830							
		1.6		1440		1700							

Table 2. Continued.

		TE	TE mean	YS	YS mean	Rm	Rm mean	HV5_1	HV5_2	HV5_3	HV5_4	HV5_5	HV5 mean
	8 Cr	2.2	**2.47**	1330	**1493**	1680	**1770**	470	434	456	438	450	**450**
		2.7		1560		1790							
		2.5		1590		1840							
	10 Cr		**4.15**	1390	**1220**	1780	**1806**	420	430	392	439	473	**431**
		3.9		1160		1780							
		4.4		1110		1860							
10 min @ 850 °C/OQ	2 Cr	1.8	**2.27**	1939	**1772**	2059	**2056**	655	487	582	641	638	**601**
1 h @ 300 °C/OQ		2.2		1951		2059							
		2.8		1425		2051							
	4 Cr	2.5	**1.83**	1954	**1716**	2038	**2013**	545	605	645	582	547	**585**
		1.4		1967		2066							
		1.6		1228		1936							
	6 Cr	2.4	**3.13**	1193	**1499**	1878	**1923**	493	526	490	528	553	**518**
		3.5		1666		1993							
		3.5		1638		1899							
	8 Cr	4.5	**2.83**	420	**1210**	1697	**1714**	451	461	493	476	441	**464**
		1.8		1590		1672							
		2.2		1620		1773							
	10 Cr	4.4	**3.40**	1523	**1250**	1708	**1695**	488	467	486	499	467	**481**
		1.9		1506		1707							
		3.9		721		1673							
10 min @ 850 °C/OQ	2 Cr	4.1	**3.33**	1360	**1447**	1670	**1586**	454	455	455	470	462	**459**
1 h @ 400 °C/OQ		2.5		1360		1440							
		3.4		1620		1650							
	4 Cr	2.5	**2.23**	1590	**1590**	1670	**1663**	479	437	438	423	430	**441**
		0.8		1630		1630							
		3.4		1550		1690							
	6 Cr	3.9	**3.23**	1490	**1547**	1640	**1626**	438	423	431	439	470	**440**
		2.6		1500		1550							
		3.2		1650		1690							
	8 Cr	4.4	**4.13**	1480	**1483**	1660	**1613**	442	435	449	435	441	**440**
		3.5		1370		1520							
		4.5		1600		1660							
	10 Cr	3.9	**4.67**	1470	**1540**	1580	**1646**	430	461	442	464	438	**447**
		5.1		1630		1680							
		5		1520		1680							
10 min @ 850 °C/OQ	2 Cr	3.3	**2.87**	1762	**1744**	2021	**2020**	698	657	660	660	662	**667**
1 h @ 500 °C/OQ		3.4		1637		2032							
		1.9		1832		2010							
	4 Cr	0.7	**2.07**	1636	**1838**	2103	**2071**	574	558	629	570	570	**580**
		2.1		1950		2047							
		3.4		1927		2063							
	6 Cr	3.8	**3.37**	1843	**1762**	1948	**1934**	516	572	551	533	501	**535**
		3.3		1701		1949							
		3		1742		1905							

1900404 (10 of 16)

Table 2. Continued.

		TE	TE mean	YS	YS mean	Rm	Rm mean	HV5_1	HV5_2	HV5_3	HV5_4	HV5_5	HV5 mean
	8 Cr	3.5	**2.40**	1426	**1555**	1766	**1730**	450	474	466	405	456	**450**
		0.4		1594		1644							
		3.3		1643		1782							
	10 Cr	2.5	**2.00**	1442	**1515**	1669	**1674**	486	461	491	474	494	**481**
		1.7		1593		1672							
		1.8		1510		1683							
10 min @ 850 °C/OQ	2 Cr	10.5	**9.80**	838	**811**	972	**927**	275	280	282	275	303	**283**
1 h @ 600 °C/OQ		9.8		808		924							
		9.1		787		885							
	4 Cr	10.9	**10.03**	789	**799**	963	**941**	268	273	269	264	271	**269**
		11		833		966							
		8.2		774		896							
	6 Cr	9.6	**11.07**	722	**750**	888	**914**	244	265	265	276	269	**264**
		13.3		772		926							
		10.3		757		928							
	8 Cr	9.2	**11.37**	694	**730**	889	**922**	248	260	252	252	264	**255**
		12.1		729		937							
		12.8		767		942							
	10 Cr	11.8	**12.70**	743	**725**	915	**941**	248	270	255	274	259	**261**
		12.6		668		959							
		13.7		764		950							
10 min @ 1150 °C/OQ	2 Cr					373	**372**	435	434	360	457	479	**433**
						394							
						351							
	4 Cr					285	**320**	498	488	533	451	535	**501**
						360							
						317							
	6 Cr					315	**298**	425	479	504	467	506	**476**
						254							
						326							
	8 Cr					318	**343**	439	430	434	445	460	**442**
						363							
						348							
	10 Cr					390	**395**	438	446	446	389	480	**440**
						366							
						430							
10 min @ 1150 °C/OQ	2 Cr	0.1	**0.10**			407	**448**	436	414	409	448	456	**433**
1 h @ 200 °C/OQ						529							
						408							
	4 Cr	0.2	**0.20**			411	**466**	501	476	483	451	384	**459**
						445							
						542							
	6 Cr	0.1	**0.10**	423	**423**	464	**501**	480	460	490	502	461	**479**
		0.2				467							
		0				574							

Table 2. Continued.

		TE	TE mean	YS	YS mean	Rm	Rm mean	HV5_1	HV5_2	HV5_3	HV5_4	HV5_5	HV5 mean
	8 Cr	0.1	**0.10**			492	**498**	511	449	473	512	536	**496**
		0.1				540							
		0.1				464							
	10 Cr	0.1	**0.13**	587	**587**	564	**601**	474	540	529	434	443	**484**
		0.1				571							
		0.2				668							
10 min @ 1150°C/OQ	2 Cr					759	**799**	526	527	528	524	560	**533**
1 h @ 300°C/OQ						802							
						838							
	4 Cr	0.1	**0.07**			949	**951**	403	494	517	460	438	**462**
		0				978							
		0.1				929							
	6 Cr	0.2	**0.33**			736	**1038**	522	467	470	431	466	**471**
		0.8				1228							
		0				1151							
	8 Cr	0.7	**1.00**	980	**971**	1430	**1497**	582	538	526	488	506	**528**
		1.3		915		1545							
		1		1019		1518							
	10 Cr	1.7	**1.47**	752	**756**	1468	**1466**	582	529	529	519	493	**530**
		1.2		674		1415							
		1.5		842		1518							
10 min @ 1150°C/OQ	2 Cr	0.2	**0.40**	1220	**1250**	1320	**1333**	414	448	461	422	367	**422**
1 h @ 400°C/OQ		1		1280		1380							
		0				1300							
	4 Cr	−0.8	**−0.13**		**589**	1390	**1171**	464	473	453	464	471	**465**
		−1				1270							
		1.4		589		853							
	6 Cr	0.1	**0.33**		**1080**		**1195**	437	456	450	445	461	**450**
		0.3		1070		1130							
		0.6		1090		1260							
	8 Cr	0.4	**0.43**	1010	**972**	1040	**1063**	449	466	437	434	458	**449**
		0.6		911		1110							
		0.3		995		1040							
	10 Cr	1	**1.77**	947	**792**	1140	**1156**	519	487	507	480	529	**504**
		1.5		856		1140							
		2.8		574		1190							
10 min @ 1150°C/OQ	2 Cr	2.3	**3.17**	1102	**1029**	1201	**1248**	430	402	372	363	435	**400**
1 h @ 500°C/OQ		2.8		1082		1268							
		4.4		905		1276							
	4 Cr	1.5	**1.90**	1313	**1197**	1456	**1458**	362	461	374	353	349	**380**
		1.4		989		1403							
		2.8		1289		1517							
	6 Cr	0.5	**0.87**	1435	**980**	1541	**1074**	445	457	474	450	453	**456**
		1.4		884		996							
		0.7		620		687							

1900404 (12 of 16)

Table 2. Continued.

		TE	TE mean	YS	YS mean	Rm	Rm mean	HV5_1	HV5_2	HV5_3	HV5_4	HV5_5	HV5 mean
	8 Cr	0.8	**0.50**	870	**1000**	1471	**1417**	690	698	731	687	670	**695**
		0.7		1131		1493							
		0				1288							
	10 Cr	1.5	**1.63**	729	**786**	1435	**1486**	522	504	491	549	528	**519**
		1.9		666		1483							
		1.5		963		1541							
10 min @ 1150 °C/OQ	2 Cr	7	**6.50**	781	**750**	950	**916**	209	272	287	291	303	**272**
1 h @ 600 °C/OQ		5.7		709		858							
		6.8		760		942							
	4 Cr	5	**4.67**	839	**847**	1060	**1041**	279	223	291	289	295	**275**
		4.1		833		975							
		4.9		868		1090							
	6 Cr	7.7	**6.77**	792	**784**	1080	**1053**	273	264	284	267	251	**268**
		6.2		762		1010							
		6.4		797		1070							
	8 Cr	6.8	**7.23**	742	**809**	1130	**1153**	318	259	283	297	294	**290**
		7.4		950		1170							
		7.5		736		1160							
	10 Cr	8.9	**8.43**	878	**860**	1220	**1200**	282	294	283	273	235	**273**
		7.5		829		1180							
		8.9		872		1200							

changes developed. We exemplarily studied samples from the Fe–0.2C–4Cr (Figure 5, left) and Fe–0.2C–8Cr (Figure 5, right) alloys oil-quenched from 1000 °C and tempered at 400 °C, followed by oil-quenching. Here, a strength difference of about 200 MPa and a ductility increase can be noted, which does not arise for any other state in this compositional range. This behavior may be related to a multitude of interacting phenomena with different weighting as a consequence of the tempering, such as rearrangement of carbon, development of carbides, or the coarsening of the lath microstructure (cf. Figure 5).[19] Even though no γ was detected in both material states, its pre-existence in the microstructure prior to tempering—thus its impact on the mechanical performance—by transformation to α' during tensile testing or metallographic preparation is conceivable.[20] Despite a detailed analysis, no explicit reasons for this unexpected material behavior can be given. Further investigations into the underlying microstructural reasons such as dislocation density, packing density of martensite laths, or prior austenite grain sizes indeed may give additional insights but may not be sufficient to fully clarify the complex reasons for materials' behavior, thus not contribute toward its understanding. In the context of high-throughput experiments, the efforts for these time-consuming in-depth experiments were deliberately kept low. Apart from microstructural analysis, these phenomena may be attributed to an unfortunate coincidence of several processing-related factors such as notches, spalling, torsion, or the bending of tested materials induced by the hot-rolling, handling, quenching, or cutting of the not standardized RAP tensile samples.

4.2. High-Throughput Design Challenges

The implementation of high-throughput methods in the material sciences typically aims for the identification of trends via correlation of rapidly generated data.[21] This requires systematic approaches in controlled conditions, which can efficiently generate simply recordable data. For conducted experiments, material properties (single data; e.g., hardness) or determined characteristic values (e.g., YS) seem to be most suitable. A broad range of parameters may be determined from tensile testing results which need to be tailored to fit materials' characteristics; e.g., material parameters such as uniform elongation may be ideally suited for soft and ductile materials, yet unusable for hard and brittle materials. The multitude of chosen descriptive material parameters (e.g., YS, UTS, TE) generated in combination with varying material compositions and states opens up multi-dimensional spaces, holding challenges for interpretation. Attempts to overcome this trade-off are multi-dimensional plots such as spider diagrams or heat-maps as shown in **Figure 6** (left: Fe–0.2C–XCr alloys; right: Fe–0.8C–XCr alloys). Here, the effect of hardening temperature (top and bottom picture), tempering temperature (x-axis), and Cr content (y-axis) on materials' mechanical performance (YS × TE; color coded) is exemplarily expressed. Consequently, every map reduces 4 dimensions (mentioned earlier) in a 2D space. Uniform color coding was used in all the maps (red: high values, black: low values) to ensure comparability. The compilation of these four heat-maps (Figure 6) gives first insights into materials' performance such as their suitability for forming applications
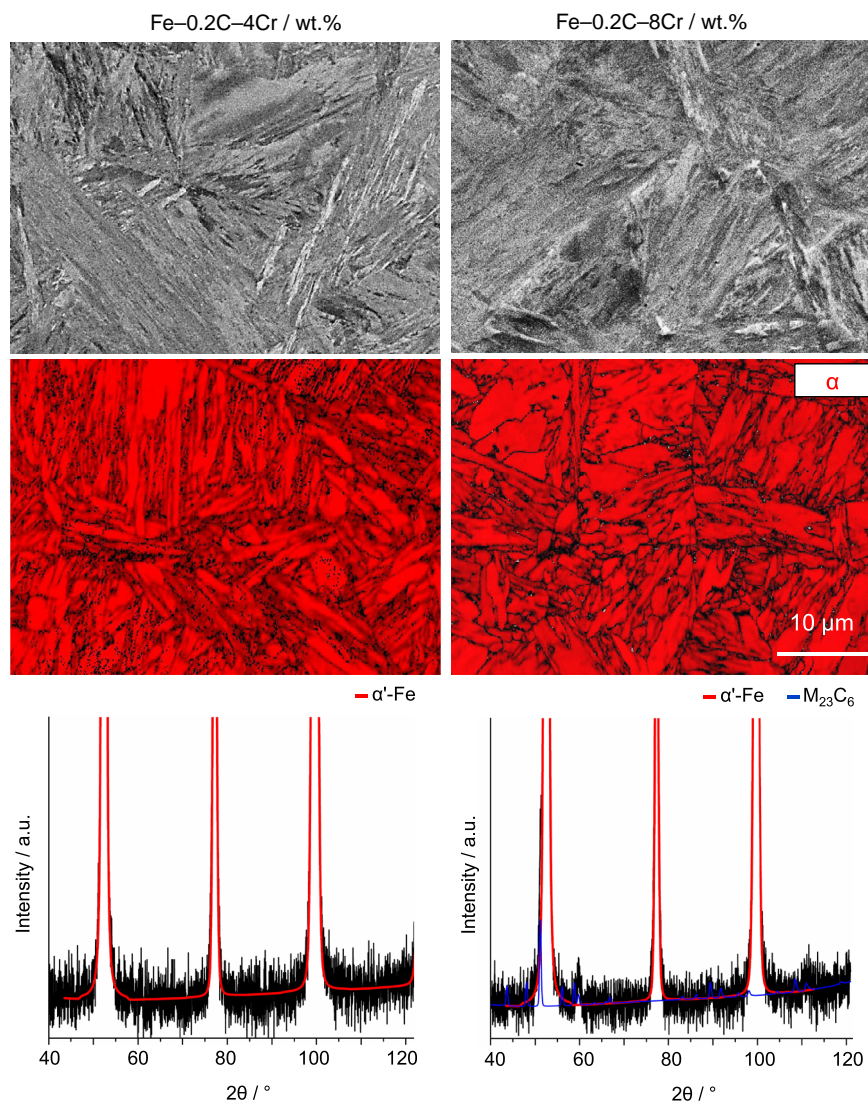
1900404 (13 of 16)

**ADVANCED
SCIENCE NEWS**
www.advancedsciencenews.com

**steel
research**
international
www.steel-research.de

Figure 5. Microstructural analysis of samples (left: Fe–0.2C–4Cr; right: Fe–0.2C–8Cr) in hardened (1000 °C/10 min/oil-quenching) and tempered (400 °C/1 h/oil-quenching) conditions. Top: SE images; middle: EBSD phase map, here image quality in grayscale is superimposed with the α'-Fe phase in red; bottom: XRD results (black) and fitting results α'-Fe (red) and $M_{23}C_6$ (blue).

(ductility) or wear resistance (hardness). However, these traditional data analysis are biased by perspectives based on empirical experience, thus offering potential missing relevant interconnections or underlying information.

4.3. Leaving Traditional Design Routes

The extension of high-throughput approaches by computer-assisted data processing and analysis open up assistance for materials science confronted with multi-dimensional problems. However, to exploit the potential of computational methods, consistent data production and data handling is required. Data are ideally simple to generate, to extract/parse (single values), and also to access (e.g., via a database) to apply data processing (algorithms). Typically, already simple experiments (such as tensile tests) deliver large quantities of data, not allowing straightforward analysis, but require the extraction of descriptive

materials parameters dependent on boundary conditions (e.g., turning points or maximum values). Further extraction of underlying information ideally utilized parsing of raw data and automatic determination of single-value parameters—possible also of unconventional nature—to avoid human errors. Subsequently, data processing (ratios, ratings, random) can assist in generating data tangible by human or alternatively artificial intelligence to reduce the complexity of these multi-dimensional problems in an iterative manner (e.g., re-set constrains).

5. Conclusions

We systematically studied the effect of various Cr additions (2, 4, 6, 8, 10 wt%) on mechanical properties and microstructures of Fe–0.2C (wt%) and Fe–0.8C (wt%) based steels depending on their hardening and tempering conditions. The following
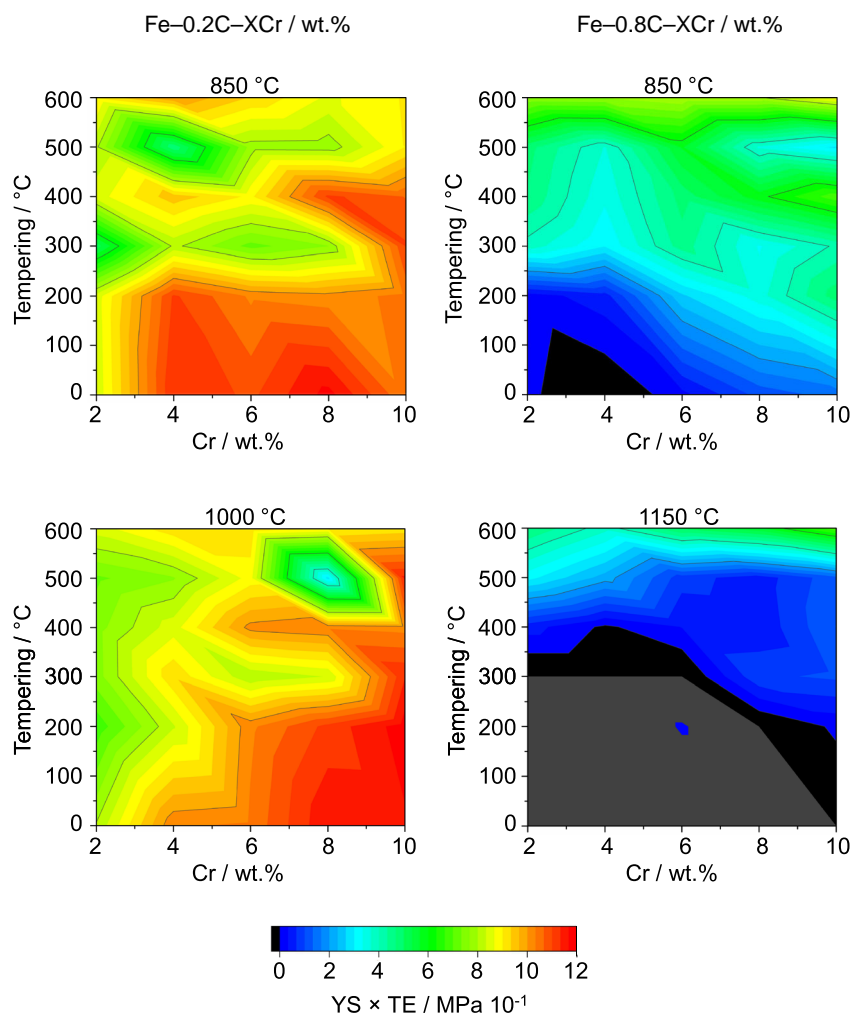
1900404 (14 of 16)

Figure 6. Color-coded heat maps revealing the effects of hardening temperature, tempering temperature, and Cr content on mechanical performance (YS × TE) of the different alloys (left: Fe–0.2C–XCr; right: Fe–0.8C–XCr). Uniform color coding was used in all the maps (red: high values, black: low values).

conclusions can be drawn: 1) The variety of states analyzed reveal a broad range of mechanical properties reaching strengths up to 1.8 GPa UTS or hardness of 700 HV5. Individual trends can be obtained while straightforward interpretation of trends holds complex analytical challenges; 2) Diversity of mechanical properties are associated with various competing phenomena influencing the materials microstructures, such as microstructures present prior to hardening or phase formation and fractions such as austenite or carbide. However, interconnections associated with their occurrence are too complex to grasp within this study, thus selected states were analyzed in-depth; 3) We discussed classical data analysis and interpretation methods such as dimension reduction via multi-axis plots/heat maps as well as the potential of assistive computational data processing, analysis, and its challenges to deal with multi-dimensional interconnections.

Conflict of Interest

The authors declare no conflict of interest.

[1] M. F. Ashby, *Materials Selection in Mechanical Design*, 3rd ed., Butterworth-Heinemann, Burlington, MA **2005**.

[2] G. Krauss, *Steels—Processing, Structure, and Performance*, 2nd ed., ASM International, Materials Park, OH **2015**.

[3] H. Berns, W. Theisen, *Eisenwerkstoffe – Stahl und Gusseisen*, Springer, Berlin, Heidelberg **2008**.

[4] F. Rapatz, F. Roll, *Kleines Lexikon Eisenwerkstoffe*, Deutsche Verlags-Anstalt, Stuttgart **1964**.

[5] D. Raabe, D. Ponge, O. Dmitrieva, B. Sander, *Scr. Mater.* **2009**, *60*, 1141.

[6] F. Hengerer, *HTM* **2002**, *57*, 144.

[7] L. Yuan, D. Ponge, J. Wittig, P. Choi, J. A. Jiménez, D. Raabe, *Acta Mater.* **2012**, *60*, 2790.

[8] H. Springer, D. Raabe, *Acta Mater.* **2012**, *60*, 4950.

[9] K. G. Pradeep, C. C. Tasan, M. J. Yao, Y. Deng, H. Springer, D. Raabe, *Mater. Sci. Eng. A* **2015**, *648*, 183.

[10] H. Springer, M. Belde, D. Raabe, *Mater. Sci. Eng. A* **2013**, *582*, 235.

[11] H. Springer, M. Belde, D. Raabe, *Mater. Des.* **2016**, *90*, 1100.

[12] T. Swarr, G. Krauss, *Metall. Trans. A* **1976**, *7*, 41.

[13] M. Umemoto, E. Yoshitake, I. Tamura, *J. Mater. Sci.* **1983**, *18*, 2893.

[14] W. C. Leslie, *Metall. Trans.* **1972**, *3*, 5.

[15] A. P. Gulyayev, *Met. Sci. Heat Treat.* **1962**, *4*, 491.

[16] M. Yamada, L. Yan, R. Takaku, S. Ohsaki, K. Miki, K. Kajikawa, T. Azuma, *ISIJ Int.* **2014**, *54*, 240.

[17] R. A. Grange, *Metall. Trans.* **1973**, *4*, 2231.

[18] C. F. Jatczak, Retained Austenite and Its Measurement by X-Ray Diffraction, SAE International **1980**, https://doi.org/10.4271/800426.

[19] D. Shtansky, K. Nakai, Y. Ohmori, *Acta Mater.* **2000**, *48*, 969.

[20] H. S. Zhao, X. Zhu, W. Li, X. J. Jin, L. Wang, H. Jiao, D. M. Jiang, *Mater. Sci. Technol.* **2014**, *30*, 1008.

[21] W. F. Maier, K. Stöwe, S. Sieg, *Angew. Chem., Int. Ed.* **2007**, *46*, 6016.